

New double beam spectrophotometer for microsamples. Application to hydrostatic pressure experiments

B. Amaya Moral and Fernando Rodríguez

Departamento CITIMAC. Facultad de Ciencias. Universidad de Cantabria. 39005 Santander, Spain

(Received 30 January 1995; accepted for publication 9 August 1995)

This article describes a new double beam spectrophotometer specially conceived for optical absorption measurements on low-absorbing microsamples. The available long-working distance makes this apparatus attractive for use on samples placed in special environments such as heating stages, biological cells, and particularly hydrostatic pressure cells. Its performance has been tested in optical absorption measurements for different Mn^{2+} and Cu^{2+} complexes. We applied the instrument for investigating the electronic spectrum of Cu^{2+} doped $(\text{CH}_3\text{CH}_2\text{NH}_3)_2\text{CdCl}_4$ crystals under hydrostatic pressure using a Sapphire anvil cell. A salient feature of this work is the enormous redshift (1400 cm^{-1}) experienced by the first $\text{Cl}^- \rightarrow \text{Cu}^{2+}$ charge transfer band at 26 kbar. We briefly comment on the origin of this shift. © 1995 American Institute of Physics.

I. INTRODUCTION

This article presents a new double beam spectrophotometer specially designed for measuring optical absorption (OA) spectra in microsamples ($\geq 50\text{ }\mu\text{m}$) at working distances of up to 2.5 cm. The aim of developing this apparatus regarding other similar existing devices,¹⁻⁸ is threefold:

(1) To improve the absorbance sensitivity down to 10^{-3} levels. This point is of great interest for obtaining OA spectra of low-absorbing materials.

(2) The apparatus must be able to operate at long working distances. This requirement primarily arose in double beam measurements under hydrostatic pressure using either diamond or sapphire anvil cells (DAC and SAC, respectively) with distances between the sample cavity and the outer cell boundary longer than 2 cm. In particular, this situation occurs in the SAC prototype^{9,10} employed in our experiments. Interestingly, this characteristic widens the applications of the present apparatus to absorption measurements in microsamples placed in special environments such as cryogenic devices, heating stages or biological cells, which necessarily impose long operation lengths.

(3) To increase the light intensity into the sample cavity as well as the detection sensitivity in order to get a fast response.

All these requirements have been met by means of a microscope equipped with reflecting optics in order to enhance the UV transmission as well as to avoid chromatic dispersion effects. The original *in situ* double beam system presented in this work consists of two optical fibers placed on the image plane of the microscope that act as diaphragms for the sample and reference beams. The transmitted light is detected through two independent photomultiplier tubes attached to the fiber ends. The proposed double beam system actually improves the absorption sensitivity because the reference and sample beams are both close and parallel as they go through the hydrostatic cavity thus providing similar pathways in contrast to other double-beam devices described elsewhere.⁶ In particular, the variations of light intensity due either to temporal fluctuations or to changes in the spectral distribution of the lamp are instantaneously corrected with

the present system. Such fluctuations are important in experiments carried out with single-beam devices given that the reference (I_0) and sample (I) signals are obtained from two independent scans. Moreover, this new procedure drastically reduces the effects associated with changes of the spatial intensity distribution in the sample cavity induced by mechanical misalignments or chromatic dispersion effects by the anvils in pressure experiments. These important aspects are only partially accounted for in Ref. 6 since the reference beam path is outside the DAC. However, the setup described in Ref. 6 is advantageous for measuring four orders of optical density from 1 to 5, in contrast to our apparatus, which is conceived for operating within a complementary low-absorbance range (0.001–1). The maximum optical density which can be measured with the present double-beam system is limited by light scattering effects from the microsample and has values of $A \leq 1$ in the more unfavorable case when operating in the UV region ($\lambda < 300\text{ nm}$). For high-absorbing materials ($A > 1$), this limitation can be, however, overcome with the present experimental setup by adapting the standard single-beam operation mode.^{4,5,8} It must be pointed out that the detection system employed in our apparatus largely improves the sensitivity of current charge couple devices (CCD). This is particularly important for weak-light intensity since the selected optical fibers directly collect the sample and reference light pencils of $20\text{ }\mu\text{m}$ of diameter and therefore the effective detection area is much larger than the corresponding CCD pixel area. This system allows us to obtain suitable signal-to-noise ratios for times of about 0.1 s.

We tested our apparatus in OA experiments on low-absorbing crystals such as $[(\text{CH}_3)_4\text{N}]_2\text{MnBr}_4$ and used it for obtaining the charge transfer (CT) spectra of $(\text{RNH}_3)_2\text{MnCl}_4$ and $(\text{RNH}_3)_2\text{CdCl}_4$ (R = methylene or ethylene) microcrystals doped with 0.4 and 0.2 mol % Cu^{2+} , respectively. Interestingly, we also measured the variation of the first CT band in $(\text{RNH}_3)_2\text{CdCl}_4$: Cu^{2+} under hydrostatic pressures up to 31 kbar, using a SAC prototype.⁹ The results indicate that the first $\text{Cl}^- \rightarrow \text{Cu}^{2+}$ CT band experiences an abrupt redshift of 1400 cm^{-1} at 26 kbar. This salient feature is interpreted in terms of changes of the local structure of the formed CuCl_6^{4-}

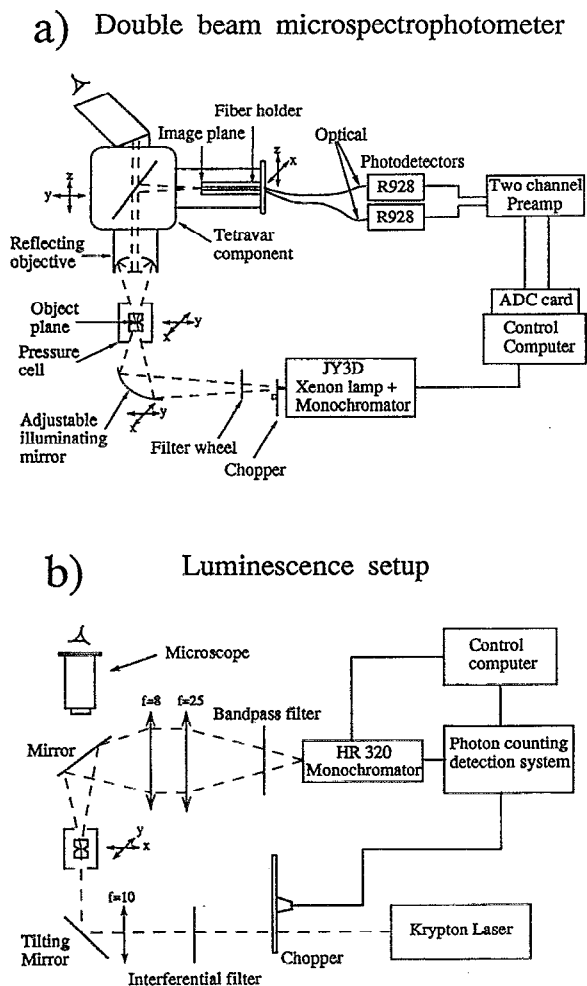


FIG. 1. Schematic drawing of (a) the micro-optical double-beam system for optical absorption measurements under hydrostatic pressure using a sapphire anvil cell and (b) the luminescence setup.

complex as consequence of a pressure-induced structural phase transition undergone by the layer perovskite.

II. EXPERIMENTAL SETUP

Figure 1(a) shows the scheme of the new double beam microspectrophotometer. We used a Jobin-Yvon JY3D fluorimeter equipped with a 150 W Xenon lamp for obtaining the monochromatic light. The light is focused onto the sample cavity with a toroidal mirror that provides a beam spot of about 0.5 mm^2 . For hydrostatic pressure experiments, the original SAC prototype⁹ was properly machined in order to improve the aperture from $f/5.0$ to $f/2.5$. The SAC (or the sample holder in case of nonpressure experiments) is mounted on a precision x - y translation stage for sample orientation. The microscope consists of an Ealing tetra-var component equipped with an Ealing $15\times$ reflecting objective and two windows for optical detection and the ocular eyepiece. The use of this objective is advantageous not only for working in the UV range avoiding chromatic dispersion, but also for working at sample distances of up to 2.5 cm. This latter aspect is essential in pressure experiments. The microscope collects and focuses the transmitted light forming a $12\times$

magnified image of the sample area. Two identical optical fibers (Mitsubishi ST-U200D-FV) of 0.20 mm core diameter placed on the back focal plane act as image delimiters [Figs. 1(a) and 2]. They transmit the selected sample and reference light beams to two Hamamatsu R928 photomultiplier tubes. The two signals are amplified and read by means of a low noise preamp and an HP 98640A analog input interface [analog-to-digital convertor (ADC) card], respectively. The experiment is fully controlled by an HP series 300 micro-computer through suitable iterative programs.

The optical fibers were placed on a homemade holder with a separation of 0.46 mm and polished with $1 \mu\text{m}$ corundum powder. The holder was mounted on an x - z fiber micropositioner to align the two fibers with selected points of the concentric circle graticule of the ocular eyepiece. Precise fiber alignments were attained by means of a $20 \mu\text{m}$ diaphragm. This fiber arrangement ensures nearly the same illumination for the two fibers and also avoids mutual interference from the sample and reference beams. This aspect is illustrated in the plot of Fig. 3 that represents the transmitted intensity through each fiber of a $20 \mu\text{m}$ diaphragm spot as a function of the spot position. Note that the intensity of fiber 2 is zero when the spot is centered on fiber 1 and vice versa. It is important to point out that a precise alignment of the incident beam with the microscope axis drastically reduces the chromatic dispersion effects induced by the sapphire anvils in pressure experiments. Figure 2 shows a schematic view of the hydrostatic cavity and the corresponding image seen through the ocular eyepiece.

The present experimental setup is able to measure absorbances in the 0.001–1 range. Although this range covers the spectroscopic needs for many materials, absorption measurements involving optical densities greater than 1 like those for band gaps in semiconductors or CT bands in concentrated compounds, can be easily performed with our apparatus by working on the single beam mode. In such a case, we used beam spots of about $30 \mu\text{m}$ of diameter by inserting another Ealing $15\times$ reflecting objective with suitable diaphragms in the illumination system. The weak-light intensity is then measured with a Stanford Research SR400 photon counter using the lock-in mode operation.

We tested the apparatus with microsamples placed on quartz plates and dipped in Merck spectroscopic paraffin oil in order to match the sample refractive index. It is worth noting that although the present apparatus covers the 240–900 nm spectral range, which is mainly imposed by both the fiber transmittance and the photomultiplier sensitivity, this range can be extended to the NIR region by proper selection of the detection system.

Figure 1(b) shows the experimental setup employed for luminescence measurements under hydrostatic pressure. The excitation beam spot is positioned within the hydrostatic cavity by two tilting mirror screws. This operation is controlled by a microscope placed above the SAC. The luminescence is collected through a collimating lens (8 cm focal) and focused into the entrance slit of a Jobin-Yvon HR 320 monochromator with a 25 cm focal lens. Suitable interference and bandpass filters are placed in the excitation and emission pathways, respectively. Standard photocounting techniques

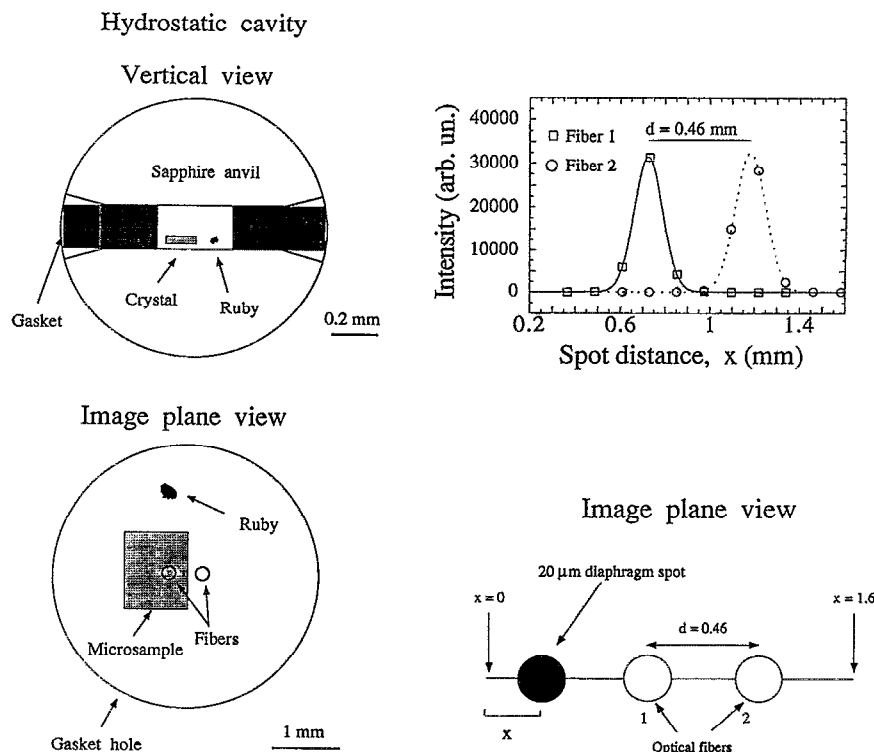


FIG. 2. Left: Vertical view of the hydrostatic cavity and arrangement of the microsample and the optical fibers in the image plane of the microscope. Right: Plot of the transmitted light intensity through fibers 1 and 2 vs spot distance in the image plane. The spot corresponding to a 20 μm diam diaphragm placed on the object plane was moved along the straight line indicated in the drawing. Full and dotted curves are Gaussian fittings of the experimental intensity for fibers 1 and 2, respectively.

were employed for light detection. Small ruby chips ($\sim 20 \mu\text{m}$) have been utilized for pressure calibration. The ruby is excited with the 530.9 nm beam of a Coherent I-302-K Krypton laser. The pressure is determined from the R_1 and R_2 line shifts through the equation:^{1,3,8} $P = 27.5 \Delta\lambda$ where P and λ are given in kbar and nm, respectively.

III. SPECTROSCOPIC MEASUREMENTS

A. Optical absorption spectra of MnBr_4^{2-} and CuCl_6^{4-} complexes

We used the apparatus in absorption measurements on single microcrystals of $[(\text{CH}_3)_4\text{N}]_2\text{MnBr}_4$ and $(\text{RNH}_3)_2\text{CdCl}_4: \text{Cu}^{2+}$ and $(\text{RNH}_3)_2\text{MnCl}_4: \text{Cu}^{2+}$. Figure 3 shows the OA spectra of these crystals obtained through the experimental setup of Fig. 1(a). Its performance is illustrated by comparing these spectra with those obtained from a standard Perkin-Elmer Lambda 9 spectrophotometer. Sample sizes are typically about $100 \times 100 \times 30 \mu\text{m}^3$ and $10 \times 10 \times 0.5 \text{mm}^3$, respectively. The good sensitivity of the apparatus is reflected in the OA spectrum of the $[(\text{CH}_3)_4\text{N}]_2\text{MnBr}_4$ crystal whose absorption peaks have optical densities lower than 0.02. However, it is worth pointing out that each OA spectrum has been obtained with two independent measurements. The first measurement provides the sample and reference intensities, $I(11)$ and $I_0(21)$, respectively, while the second one gives two reference intensities, $I_0(12)$ and $I_0(22)$, near to the sample area, within the cavity (the numbers in parenthesis

denote the fiber number and the spectrum number, respectively). The latter spectrum is employed to correct the slightly different wavelength-dependent response of the two independent photomultiplier tubes. The absorbance is thus given by

$$A = \log \left[\frac{I_0(21)/I_0(22)}{I(11)/I_0(12)} \right] = \log \left[\frac{I_0(21)I_0(12)}{I(11)I_0(22)} \right] \quad (1)$$

This procedure improves the sensitivity of the OA spectra down to 10^{-3} . Figure 4 shows the efficiency of this method by comparing the effect of correction in the zero absorption background and the OA spectrum of the $(\text{RNH}_3)_2\text{MnCl}_4: \text{Cu}^{2+}$ crystal. The uncorrected spectra were obtained through one simple scan using the $I_0(11)$ and $I_0(21)$ intensities for the background, and $I(11)$ and $I_0(21)$ for the crystal spectrum, whereas the corrected spectra were obtained from Eq. (1) using the background correction intensities $I_0(12)$ and $I_0(22)$. Note that the two zero absorption spectra required to obtain the corrected zero background were taken in two different regions of the sample cavity. We obtained a zero background accuracy better than 10^{-4} in the whole spectral region if the two zero absorption spectra were taken at the same position.

The quality of the spectra obtained with this setup is worth noting, taking into account that we only used a Xenon lamp at variance with standard spectrophotometers which are usually equipped with tungsten and deuterium lamps for covering the whole spectral range. As shown in Fig. 4, our

Double beam absorption setup Standard spectrophotometer

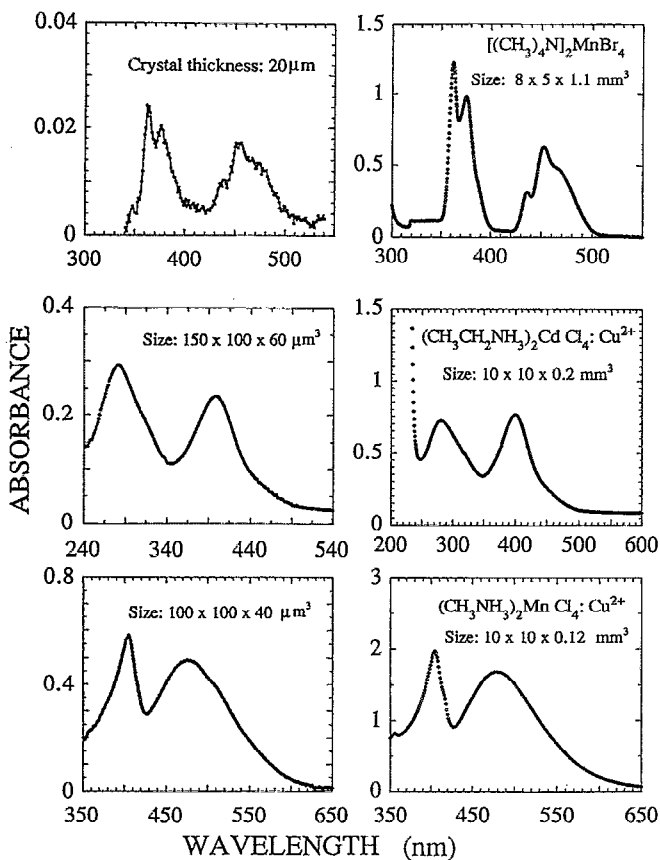


FIG. 3. Room temperature optical absorption spectra of different Mn^{2+} and Cu^{2+} systems obtained with the present apparatus (left) and with a standard spectrophotometer (right). The crystal size is indicated in each case. Spectral resolution: $\Delta\lambda=4$ nm. The time response was 0.1 s, except for the Mn crystal ($t=0.5$ s) and the $(RNH_3)_2CdCl_4: Cu^{2+}$ crystal in the 240–340 nm range ($t=1$ s).

double-beam system fully avoids the presence of disturbances in the Xe peak region around 480 nm.

A detailed analysis of the OA spectra of Fig. 3 is given elsewhere.^{11–13}

B. Variation of the charge transfer spectra of $(RNH_3)_2CdCl_4: Cu^{2+}$ under hydrostatic pressure

We employed our apparatus to investigate the pressure dependence of the first $Cl^- \rightarrow Cu^{2+}$ CT band in $(RNH_3)_2CdCl_4: Cu^{2+}$. Figure 5 shows the evolution of the optical absorption spectra of this crystal with pressure. The corresponding ruby luminescence spectra as a pressure probe are also included. The presence of R-lines from unavoidable Cr^{3+} impurities of the sapphire anvils can be used as an atmospheric pressure indicator. It must be noted that as the pressure increases, the spectrum baseline slightly decreases towards shorter wavelengths as a consequence of the enhancement of the light-scattering processes in the UV region. With regard to the spectra of Fig. 5, two important facts must be underlined:

(1) The absorption band at 398 nm does not experience significant variations from atmospheric pressure to 25 kbar.

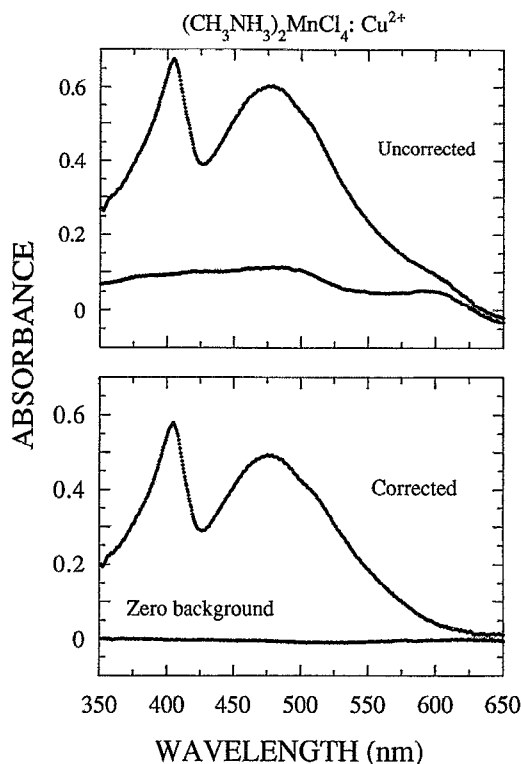


FIG. 4. Effect of the zero absorption correction on the OA spectrum of a $(RNH_3)_2MnCl_4: Cu^{2+}$ microcrystal and the zero background. The uncorrected spectra were simply obtained from a single scan, whereas the corrected ones were compensated for detection response (see text for explanation).

(2) Above this pressure, the CT band abruptly shifts to lower energies. Figure 6 plots the peak energy of this band versus pressure.

The enormous shift of -1400 cm^{-1} observed at 26 kbar is worth pointing out. This strong variation is associated with the occurrence of a structural phase transition in the host

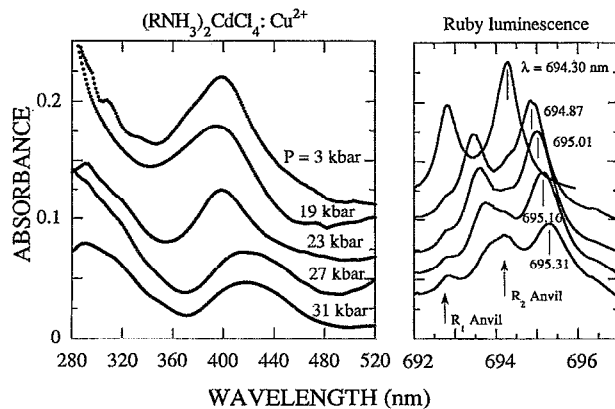


FIG. 5. Pressure dependence of the OA spectrum of $(RNH_3)_2CdCl_4: Cu^{2+}$. Sample size: $110 \times 80 \times 33$ μm^3 . The corresponding ruby luminescence is shown on the right side. The arrows indicate the Cr^{3+} signals coming from the sapphire anvils. The hydrostatic pressures of the left-hand graph were obtained from the corresponding R_2 line of the ruby through the equation: $P=27.5 \Delta\lambda$, where $\Delta\lambda=\lambda-694.18$. Each value of λ is indicated in the graph.

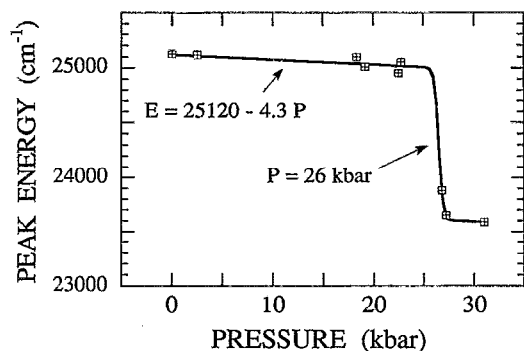


FIG. 6. Variation of the peak energy of the first CT band of $(\text{RNH}_3)_2\text{CdCl}_4:\text{Cu}^{2+}$ with pressure. The curve corresponds to an empirical function for describing the peak shift. Note the abrupt jump of -1400 cm^{-1} at 26 kbar. Below 25 kbar, the linear variation of the peak energy is given by the equation: $E\text{ (cm}^{-1}\text{)}=25120-4.3 P$ (kbar).

crystal. This fact is in agreement with the structural phase transition sequence undergone by the $\text{NH}_3\text{C}_n\text{H}_{2n}\text{NH}_3\text{MCl}_4$ and $(\text{C}_n\text{H}_{2n+1}\text{NH}_3)_2\text{MCl}_4$ ($M=\text{Cd, Mn, Fe}$) crystal families with temperature,^{14,15} that reflects the instability of the perovskite type structure.

The present results point out the adequacy of the present double system to perform OA measurements under hydrostatic pressure employing microcrystals with optical densities of about 0.1.

ACKNOWLEDGMENTS

One of the authors (FR) is indebted to Professor H. Güdel for introducing him in hydrostatic pressure techniques

during his stay at the University of Bern and the collaboration in this field. The author also thanks Dr. H. Riesen for helpful discussions and the scientific support for using SAC. The authors are indebted to Dr. P. S. May and Dr. M. C. Marco de Lucas for their valuable advice on the apparatus design and to L. Echandia for mechanical assistance. Financial support from Caja Cantabria, the Vicerrectorado de Investigación of the University of Cantabria and the CICYT (Project No. PB92-0505) is acknowledged.

- ¹J. D. Barnett, S. Block, and G. J. Piermarini, *Rev. Sci. Instrum.* **44**, 1 (1973).
- ²J. R. Ferraro and L. J. Basile, *Appl. Spectrosc.* **28**, 505 (1974).
- ³G. J. Piermarini and S. Block, *Rev. Sci. Instrum.* **46**, 973 (1975).
- ⁴B. Welber, M. Cardona, C. K. Kim, and S. Rodríguez, *Phys. Rev. B* **12**, 5729 (1975).
- ⁵B. Welber, *Rev. Sci. Instrum.* **47**, 183 (1976).
- ⁶K. Syassen and R. Sonnenschein, *Rev. Sci. Instrum.* **53**, 644 (1982).
- ⁷B. A. Weinstein, R. Zallen, M. L. Slade, and J. C. Mikkelsen, *Phys. Rev. B* **25**, 781 (1982).
- ⁸A. Jayaraman, *Rev. Mod. Phys.* **55**, 65 (1983).
- ⁹H. Riesen, Ph.D. thesis, University of Bern, 1987.
- ¹⁰H. Riesen, U. Kindler, and H. U. Güdel, *Rev. Sci. Instrum.* **58**, 1122 (1987).
- ¹¹U. Schmid, H. U. Güdel, and R. D. Willet, *Inorg. Chem.* **21**, 2977 (1982).
- ¹²B. Baticle, F. Rodríguez, and R. Valiente, *Radiation Effects and Defects in Solids* (in press).
- ¹³M. C. Marco de Lucas and F. Rodríguez, *J. Phys. Condensed Matter* **5**, 2625 (1993).
- ¹⁴W. Depmeier, J. Felsche, and G. Wildermurth, *J. Solid State Chem.* **21**, 57 (1977).
- ¹⁵R. Kind, S. Plesko, P. Gunter, J. Roos, and J. Fousek, *Phys. Rev. B* **23**, 5301 (1981).